RNA–Ligand Interactions

DOI: 10.1002/anie.201001339

Highly Modular Structure and Ligand Binding by Conformational Capture in a Minimalistic Riboswitch**

*Elke Duchardt-Ferner, Julia E. Weigand, Oliver Ohlenschläger, Sina R. Schmidtke, Beatrix Suess, and Jens Wöhnert**

Dedicated to Professor Horst Kessler on the occasion of his 70th birthday and to Professor Christian Griesinger on the occasion of his 50th birthday

Riboswitches are highly structured RNA motifs with gene regulatory activity located in the untranslated regions of mRNAs.[1] They either modulate transcription termination or translation initiation through conformational changes triggered by direct interactions with small metabolite ligands.

Many naturally occurring riboswitches are large and structurally very complex. In contrast, synthetic riboswitches—tailored gene regulatory elements for synthetic biology applications—are based on small in vitro selected RNA aptamers.[2] Yet, despite a ligand affinity and specificity comparable to their natural counterparts only a few in vitro selected aptamers are regulatory active in vivo.[3] Recently, Suess et al. engineered a riboswitch for the aminoglycoside antibiotic neomycin B by subjecting an in vitro SELEX-pool to an in vivo screening for gene regulatory activity in a yeast-based reporter gene assay.[2b] The resulting neomycin B and ribostamycin (Figure 1a) responsive RNA-element (N1) contains only 27 nucleotides in a bulged hairpin secondary structure (Figure 1b)—the smallest riboswitch functional in vivo identified to date. In sequence and secondary structure, N1 differs completely from an in vitro selected but regulatory inactive RNA-aptamer for the same ligand (R23).[4] Instead it partially resembles the ribosomal A-site, the natural target for aminoglycoside antibiotics (Figure 1b).

[*] Dr. E. Duchardt-Ferner, S. R. Schmidtke, Prof. Dr. J. Wöhnert
Institute for Molecular Biosciences, Center for Biomolecular Magnetic Resonance (BMRZ), Johann-Wolfgang-Goethe-University Frankfurt
Max-von-Laue-Strasse 9, 60438 Frankfurt (Germany)
Fax: (+49) 69-798-29527
E-mail: woehnert@bio.uni-frankfurt.de
Dr. J. E. Weigand, Prof. Dr. B. Suess
Institute for Molecular Biosciences
Johann-Wolfgang-Goethe-University Frankfurt
Max-von-Laue-Strasse 9, 60438 Frankfurt (Germany)
Dr. O. Ohlenschläger
Leibniz-Institute for Age Research (Fritz-Lipmann-Institute), Biomolecular NMR-Spectroscopy
Beutenbergstrasse 11, 7740 Jena (Germany)

[**] This work was supported by Aventis Foundation endowed professorships in Chemical Biology to B.S. and J.W., the Deutsche Forschungsgemeinschaft (DFG) (grants WO 901/1-2 to J.W. and SU 402/4-1 to B.S.) and the Center for Biomolecular Magnetic Resonance (BMRZ) of the Johann-Wolfgang-Goethe-University Frankfurt.

Supporting information for this article is available on the WWW under http://dx.doi.org/10.1002/anie.201001339.

The NMR spectroscopic analysis of the N1 riboswitch complexed with ribostamycin identifies structural determinants for its regulatory activity and suggests a ligand binding mechanism based on conformational capture. Our results provide insights into the modularity of ligand binding sites in RNA and highlight structural and dynamic features N1 shares with the larger naturally occurring riboswitches as well as with other regulatory active aptamers. This knowledge may guide the future design of novel synthetic riboswitches for targeted in vivo applications.

Structure of the N1–ligand complex—the "OFF"-state of the riboswitch:

N1 represses gene expression upon binding to either neomycin B or the closely related but smaller ribostamycin.[2b] NMR spectra of N1 bound to either ligand (Supporting Information Figure S1) indicate that both complexes are formed with similarly high affinity and display a high degree of structural similarity suggesting that the contribution of ring IV of neomycin to the interaction is negligible. Thus, we determined the structure of the N1–ribostamycin complex, because of its superior spectral resolution for the ligand resonances, by NMR spectroscopy (see Table 1). Chemical shift assignments and coordinates have been deposited (BMRB code: 16609, pdb-code: 2kxm).[5]

The structure of ribostamycin-bound N1 consists of a continuous helical stem with canonical stacking interactions between the G5:C23 and the G9:C22 base pair despite the presence of a flexible three-nucleotide bulge (C6–U8) and a compactly folded apical hexaloop organized around a U-turn motif (U14–A16) closed by the U13:U18 base pair (Figure 1c–e).

Ribostamycin rings I and II are sandwiched between the N1 major groove, in the region from G5:C23 to U13:U18 and A17 protruding from the apical loop (Figure 2). Ring III is located close to the backbone of the 3′-strand (U18 to G20). Simultaneous contacts of the ligand with the G5:C23 base pair below and G9:C22 above the bulge (Figure 2b) clamp together the lower and upper helical stem and thus enforce the uninterrupted coaxial helical stacking across the flexible C6–U8 internal bulge. The bulge itself is not interacting with the ligand. A detailed structural description of the N1–ribostamycin complex is given in the Supporting Information.

A comparison of the N1–ribostamycin complex with other aminoglycoside binding RNAs reveals partial similarities to known aminoglycoside binding sub-motifs: The helical stem centered at the U10:U21 base pair is similar to the ribosomal

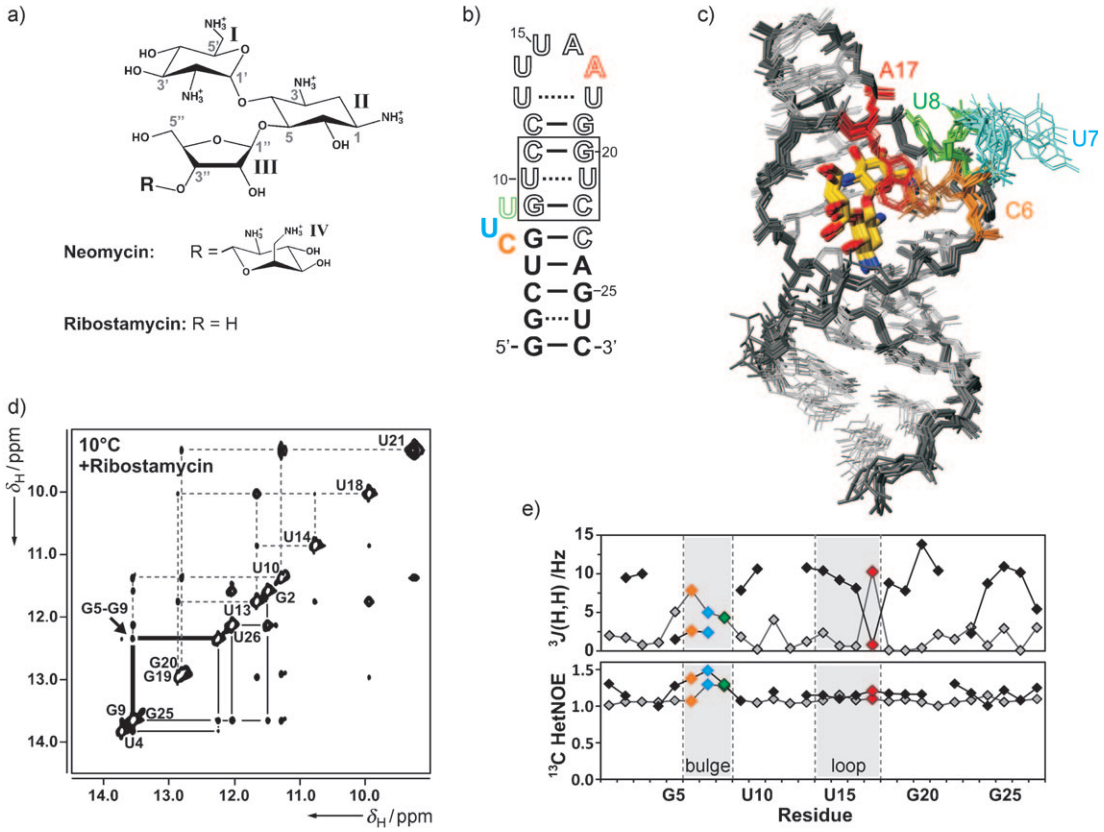

Figure 1. Structure of the N1–ribostamycin complex. a) Constitution of the 2′-deoxystreptamine class antibiotics neomycin B and ribostamycin. b) Sequence and the NMR-spectroscopy-derived secondary structure of ribostamycin-bound N1. The consensus sequence from the in vivo selection experiment for regulatory active neomycin riboswitches (U8–C23) is shown in open type face. The sequences identical to the ribosomal A-site are highlighted by a box.[2b] Bulge residues and A17 in the loop are color coded. c) NMR structural bundle, overlay of the 10 lowest energy structures. Residues are colored as in (b); ribostamycin is colored: red O, blue N, yellow C. d) Imino proton region from a 2D-[^{1}H,^{1}H]-NOESY spectrum of N1 bound to ribostamycin at 10 °C. NOE connectivity networks are indicated by solid (G2 to G5), bold (G5 to G9), and dashed lines (G9 to U21). The NOE between G5 and G9 (arrow) indicates coaxial stacking. e) Dynamics of ribostamycin-bound N1. ^{3}J(H,H) coupling constants (top) and ^{13}C HetNOE values (bottom). Bulge and loop residues are shaded in gray and colored as in (b). A large ^{3}J(H1′,H2′) coupling (gray) and a small ^{3}J(H3′,H4′) coupling (black) for A17 are indicative of a C2′-endo ribose conformation; G5 to U8 are in conformational exchange. ^{13}C HetNOE values of nucleobase C6/8 (gray) and ribose C1′ moieties (black) are indicative of a flexible internal bulge, while the apical loop is rigid.

Table 1: NMR spectroscopy and refinement statistics for the 10 lowest energy structures of the N1–ribostamycin complex.

NMR restraints		
Total distance restraints		915
N1 RNA		718
	Intra-residue	362
	Sequential	186
	Long-range	120
	Hydrogen bond	50
Ribostamycin		63
N1–Ribostamycin		134
Total dihedral restraints		106
Ribose sugar		48
Backbone		58
Structural statistics		
Pair wise RMSD values [Å]		
	N1–Ribostamycin (all residues)	0.90 ± 0.33
	N1–Ribostamycin (G2–G5, G9–U26)	0.54 ± 0.20
	Ribostamycin	0.04 ± 0.02

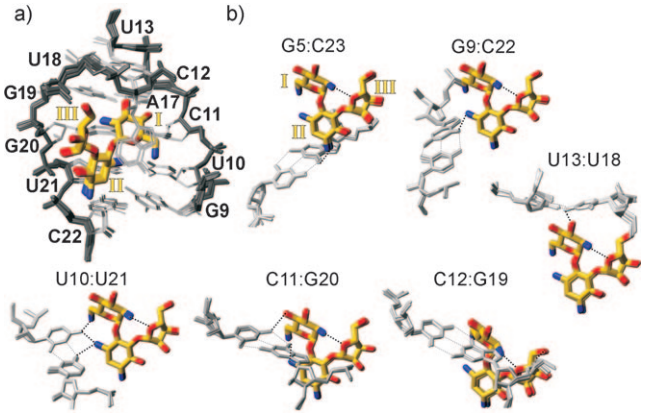

Figure 2. N1-ribostamycin interface. a) Alignment of ribostamycin in the binding pocket. Overlay of the 10 lowest energy structures. b) N1 residues interacting with ribostamycin. Intramolecular (gray dotted lines) and intermolecular (black dotted lines) hydrogen bonds or electrostatic interactions that are compatible with the calculated structure are indicated.

A-site (Supporting Information, Figure S7A).[6] Despite limited sequence homology the U-turn containing apical loop structurally resembles two in vitro selected tobramycin aptamers (Supporting Information, Figure S7B).[7] Finally, the looped-out A17 stacking onto ring I is found with the same C2′-*endo* sugar conformation and anti-base orientation in the otherwise structurally unrelated pentaloop of R23 in complex with neomycin (Supporting Information, Figure S7C).[4a] Despite these structural similarities the details of the RNA–ligand interactions in N1 differ from those observed for the other motifs (Supporting Information, Figure S8). Thus, the high ligand affinity of N1 apparently is the result of a modular combination of different aminoglycoside binding sub-motifs (Supporting Information, Figure S7D) with the detailed mode of RNA–ligand interactions for each sub-motif adapted for optimal affinity.

The "ON"-state of N1—a dynamic equilibrium:

In the absence of ligand, N1 allows the expression of its target genes. In this state, imino proton 1D and 2D NOESY spectra at temperatures above 10 °C (Figure 3a, Supporting Information, Figure S9) contain only a few narrow signals indicating an open structure (Figure 3b, left) with a five base pair lower helix (G1:C27–G5:C23) and a shortened upper helix with only two base pairs (C11:G20 and C12:G19). The apical loop and the G9:C22 as well as the U10:U21 base pair of the upper helix are destabilized. However, at lower temperatures additional imino resonances with chemical shifts typical for both Watson–Crick and non-canonical base pairs appear (Figure 3a). At −6 °C the 1D-^{1}H spectrum of free N1 and the observed NOE contacts (Figure 3c) strongly resemble those of the N1–ribostamycin complex at higher temperatures. In particular, the upper helix is extended by two additional base pairs (G9:C22 and U10:U21) and coaxial stacking between the upper and the lower helix is indicated by an NOE between the G5 and G9 imino protons. Furthermore, the apical loop folds forming the U13:U18 base pair and the U-turn with its characteristic hydrogen bond between the U14 imino group and the phosphate backbone. Thus, free N1 is in a temperature-dependent conformational equilibrium between an open form (or an ensemble of different open conformations) and a compact, highly structured conformation strongly resembling its ligand-bound state (Figure 3b).

The presence of the "bound" conformation within the conformational ensemble of free N1 suggests a conformational capture aminoglycoside binding mechanism, where the ligand selects the preformed bound conformation from the conformational ensemble of the free RNA. This mechanism constitutes an emerging alternative to an induced-fit binding mode for protein–ligand interactions and has been recently reported also for RNA–ligand systems.[8] In the free RNA, the enthalpically favored base-paired, stacked conformer resembling the bound state is largely disfavored at higher temperatures compared to the entropically advantageous open conformer(s). Ligand binding apparently overrides this entropic penalty by providing enthalpically favorable intermolecular interactions. The marked free-energy difference between the exceptionally stable complex and the conformational ensemble of the free RNA is the putative basis for the function of the neomycin-sensing riboswitch as a ligand-stabilized roadblock for the scanning ribosome in the 5′-untranslated region of the mRNA and thereby for its gene regulatory activity.

One key determinant for the destabilization of the compact state of free N1 appears to be the C6–U8 bulge which interferes with the coaxial stacking of the lower and the upper helix and the stability of their terminal base pairs. This situation would provide a functional rationale for its partial conservation within the pool of in vivo selected regulatory-active sequences despite its lack of interactions with the ligand.[2b] The destabilizing effect of the bulge is overcome by

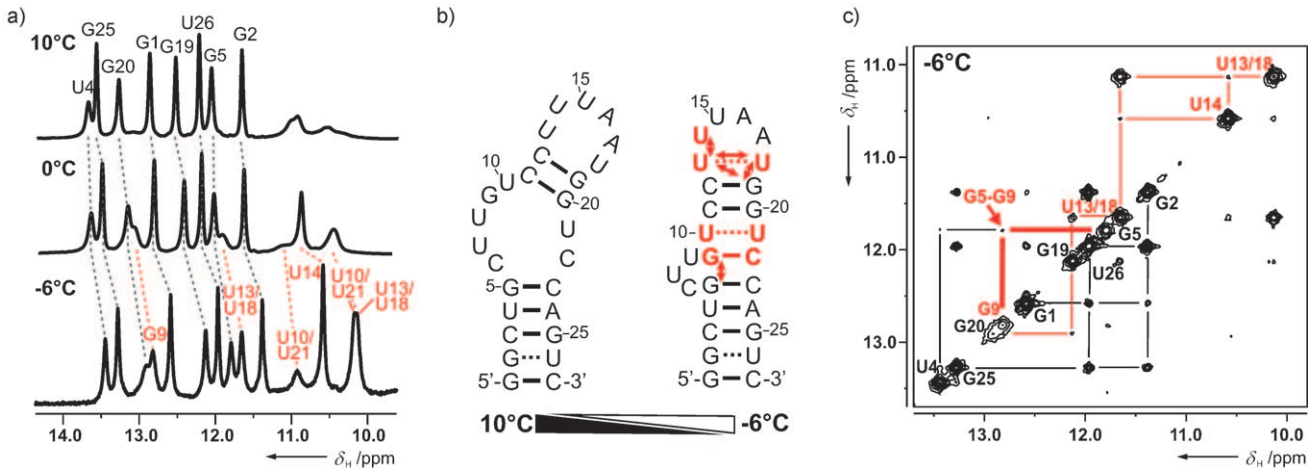

Figure 3. Temperature-dependent conformational equilibrium of free N1. a) Imino region of 1D-^{1}H NMR spectra at different temperatures. All residues giving rise to sharp imino signals at 10 °C are annotated in the spectrum. Residues emerging with higher intensity at lower temperatures are indicated in red in the spectrum recorded at −6 °C. Chemical shift changes are traced by dotted lines. b) Temperature-dependent secondary-structure changes. Residues for which an imino resonance signal emerges at lower temperature and newly formed base pairs are shown in red. New NOE connectivities are indicated by arrows. c) Imino region of a 2D-[^{1}H,^{1}H]-NOESY at −6 °C. NOE connectivity networks present at 10 °C are traced by black lines and those emerging at lower temperatures are traced by red lines. The NOE (arrow) signifying coaxial stacking between G5 and G9 (bold lines) is indicated.

ligand-induced stabilization of the U10:U21 and the G9:C22 base pairs in the upper helix as well as coaxial helical stacking by a simultaneous interaction with the G5:C23 base pair in the lower helix. In addition, ligand binding favors the folded conformation of the apical loop through stabilization of the U13:U18 base pair and through hydrophobic interactions between the ligand with A17. Ligand-enforced simultaneous stabilization of multiple structural elements and ligand-promoted interactions between these structural elements are also observed for many natural riboswitches.[1b] In particular, the relative positioning of two helical elements with respect to each other through simultaneous interactions with the ligand is reminiscent of the ligand-binding mode, for example, in the natural thiamine pyrophosphate riboswitch where a bipartite ligand enforces interhelical packing and in the preQ$_1$ riboswitch where the ligand mediates coaxial helical stacking.[9]

Remarkably, the NMR spectroscopic data for other aptamers with confirmed riboswitch activity, namely the malachite green and the theophylline aptamer, also show an open, less-structured ground state and a highly structured ligand-bound state.[3a,b,8e,10] Similar to the internal bulge in N1 the structures of these aptamer complexes reveal dynamic residues located in their ligand binding core which neither interact directly with the ligand nor contribute to complex stabilization. It is intriguing to speculate that although not selected for this purpose, these residues convey riboswitch function by promoting an open free form of the RNA. Thus, the interplay between an open ground state and a highly structured, high-affinity ligand-bound state appears to be an important determinant for the regulatory activity of both natural and synthetic riboswitches.

Received: March 5, 2010
Revised: April 29, 2010
Published online: July 14, 2010

Keywords: aminoglycosides · molecular recognition · NMR spectroscopy · riboswitches · RNA

[1] a) A. Serganov, *Curr. Opin. Struct. Biol.* **2009**, *19*, 251 – 259; b) A. Roth, R. R. Breaker, *Annu. Rev. Biochem.* **2009**, *78*, 305 – 334; c) A. D. Garst, R. T. Batey, *Biochim. Biophys. Acta Gene Regul. Mech.* **2009**, *1789*, 584 – 591.

[2] a) G. Werstuck, M. R. Green, *Science* **1998**, *282*, 296 – 298; b) J. E. Weigand, M. Sanchez, E. B. Gunnesch, S. Zeiher, R. Schroeder, B. Suess, *RNA* **2008**, *14*, 89 – 97; c) S. Topp, J. P. Gallivan, *ACS Chem. Biol.* **2010**, *5*, 139 – 148.

[3] a) D. Grate, C. Wilson, *Bioorg. Med. Chem.* **2001**, *9*, 2565 – 2570; b) I. Harvey, P. Garneau, J. Pelletier, *RNA* **2002**, *8*, 452 – 463; c) B. Suess, S. Hanson, C. Berens, B. Fink, R. Schroeder, W. Hillen, *Nucleic Acids Res.* **2003**, *31*, 1853 – 1858.

[4] a) L. Jiang, A. Majumdar, W. Hu, T. J. Jaishree, W. Xu, D. J. Patel, *Structure* **1999**, *7*, 817 – 827; b) M. G. Wallis, U. von Ahsen, R. Schroeder, M. Famulok, *Chem. Biol.* **1995**, *2*, 543 – 552.

[5] S. R. Schmidtke, E. Duchardt-Ferner, J. E. Weigand, B. Suess, J. Wöhnert, *Biomol. NMR Assignments* **2010**, *4*, 115 – 118.

[6] B. Francois, R. J. Russell, J. B. Murray, F. Aboul-ela, B. Masquida, Q. Vicens, E. Westhof, *Nucleic Acids Res.* **2005**, *33*, 5677 – 5690.

[7] a) L. Jiang, D. J. Patel, *Nat. Struct. Biol.* **1998**, *5*, 769 – 774; b) L. Jiang, A. K. Suri, R. Fiala, D. J. Patel, *Chem. Biol.* **1997**, *4*, 35 – 50.

[8] a) N. Leulliot, G. Varani, *Biochemistry* **2001**, *40*, 7947 – 7956; b) H. M. Al-Hashimi, *ChemBioChem* **2005**, *6*, 1506 – 1519; c) Q. Zhang, X. Sun, E. D. Watt, H. M. Al-Hashimi, *Science* **2006**, *311*, 653 – 656; d) Q. Zhang, A. C. Stelzer, C. K. Fisher, H. M. Al-Hashimi, *Nature* **2007**, *450*, 1263 – 1267; e) F. M. Jucker, R. M. Phillips, S. A. McCallum, A. Pardi, *Biochemistry* **2003**, *42*, 2560 – 2567; f) B. F. Volkman, D. Lipson, D. E. Wemmer, D. Kern, *Science* **2001**, *291*, 2429 – 2433.

[9] a) D. J. Klein, T. E. Edwards, A. R. Ferre-D'Amare, *Nat. Struct. Biol.* **2009**, *16*, 343 – 344; b) M. Kang, R. Peterson, J. Feigon, *Mol. Cell* **2009**, *33*, 784 – 790; c) R. C. Spitale, A. T. Torelli, J. Krucinska, V. Bandarian, J. E. Wedekind, *J. Biol. Chem.* **2009**, *284*, 11012 – 11016; d) A. Serganov, A. Polonskaia, A. T. Phan, R. R. Breaker, D. J. Patel, *Nature* **2006**, *441*, 1167 – 1171; e) S. Thore, M. Leibundgut, N. Ban, *Science* **2006**, *312*, 1208 – 1211; f) K. Lang, R. Rieder, R. Micura, *Nucleic Acids Res.* **2007**, *35*, 5370 – 5378.

[10] a) G. R. Zimmermann, R. D. Jenison, C. L. Wick, J. P. Simorre, A. Pardi, *Nat. Struct. Biol.* **1997**, *4*, 644 – 649; b) J. Flinders, S. C. DeFina, D. M. Brackett, C. Baugh, C. Wilson, T. Dieckmann, *ChemBioChem* **2004**, *5*, 62 – 72.

